

# On Estimating Local Climate Sensitivity

S.C. Chapman<sup>1</sup>, D. A. Stainforth<sup>2,1</sup>, N. W. Watkins<sup>3,1</sup>

<sup>1</sup>*Physics Department, University of Warwick, UK;* <sup>2</sup>*Grantham Institute, London School of Economics, UK;* <sup>3</sup>*British Antarctic Survey, Cambridge, UK*

Climate sensitivity is commonly taken to refer to the equilibrium change in the annual mean global surface temperature following a doubling of the atmospheric carbon dioxide concentration[1]. Evaluating this variable remains of significant scientific interest but its global nature makes it largely irrelevant to many areas of climate science, such as impact assessments, and also to policy in terms of vulnerability assessments and adaptation planning[2, 6]. Here we focus on local changes and on the way observational data can be analysed to inform us about how local climate has changed since the middle of the 19th century. Taking the perspective of climate as a constantly changing distribution we evaluate the relative changes between different quantiles of such distributions and between different geographic locations for the same quantiles. We show how the observational data can provide guidance on the sensitivity of local climate at the specific thresholds relevant to particular impact or policy endeavors. This also quantifies the level of detail needed from climate models if they are to be used as tools to assess climate change impact. The mathematical basis is presented for two methods of extracting these local sensitivities from the data. The two methods are compared using first surrogate data, to clarify the methods and their sensitivities, and then observational surface temperature timeseries from across Europe.

**Key words:** climate change, local climate sensitivity, uncertainty, prediction, impacts.

...:

## 1. Introduction

That increases in atmospheric greenhouse gases will lead to global warming and climate disruption at a level which poses a threat to society is clear. The amount of warming to expect on a global scale during the 21st century under any particular concentration scenario is, however, uncertain. It depends partly on climate sensitivity which is defined as the equilibrium change in the annual mean global surface temperature following a sustained doubling of the atmospheric carbon dioxide concentration [1]. For any given change in global mean temperature a wide variety of changes are possible at local scales. Yet it is at local scales that the impacts of climate change will be felt directly and at which adaptation planning decisions must be made [2]. Many planners and environmental disciplines are aware that an assumption of stationarity is ill-founded and therefore basing decisions on climatic distributions over the last century is likely to be sub-optimal for the climate of today and even more so for the climate of the future [3]. The question for planners is how to obtain better information to support their

assessments and decisions. The simulations of complicated global climate models can suffer from serious questions of robustness and reliability[5, 8, 7] and are known to inadequately represent behaviour which will have impact on local scales, and are therefore a questionable basis for decision making[5, 6, 2]. Our aim herein is to present an alternative; a method for analysing local climatic timeseries data to evaluate which quantiles of the local climatic distribution demonstrate the greatest sensitivity to the global changes experienced over the last 60 years. This local sensitivity automatically incorporates the effects of wider regional and global changes while allowing for the local geographic factors which affect the local climate. When combined with more generic climatic trends expected for the future, where such trends can be identified and understood, this local sensitivity provides a basis for prioritising adaptation projects and making judgements over the relative risks of different options.

As conventionally defined, climate sensitivity is the global change with respect to a fixed forcing, doubling atmospheric CO<sub>2</sub>. The local sensitivities presented herein are also changes with respect to a fixed forcing; in our case the change in climate between the 1950s and the last decade. For a mathematical audience a definition based on the derivative with applied forcing would be more appropriate. A definition based on the derivative is easily extracted from the analysis below but is not useful for the analysis of timeseries of real climatic data. For reasons similar to those which led to widespread use of the term definition of "climate sensitivity", the practicalities of climate data analysis require the evaluation to be performed on fixed, not small, changes.

We consider local climate as a distribution of some particular variable or combination of variables. Local climate change is then a change in this distribution. This change may or may not be representable by a change in the mean and/or a few higher moments of the distribution. Given the nonlinear nature of the system we might expect that it would not. A further difficulty is that variations in the distribution can occur on a wide range of timescales. The mathematical challenge is therefore to make best use of the data to quantify the changes, to identify when the change can not be well quantified and to identify the robust aspects of the results. This paper addresses these challenges.

Section two describes the mathematical foundation of the local sensitivity concept and two methods for extracting it from timeseries data. In section three the methods are illustrated using surrogate climate data designed to illustrate the concepts and the challenges of extracting a clear signal given natural climatic variations. Section four illustrates its application to real data while the conclusions present opportunities for further development and application of the technique. Further illustrations of the consequences of this technique with observed data are presented in Stainforth et al 2012 [9]. The relationship to, and representation of, the local sensitivity in terms of return times is covered in the appendix.

## 2. Method: a sensitivity parameter

Our starting point is that we have a daily observation of some variable, say mean or maximum or minimum temperature,  $T$  at different geographical locations and over an extended interval of time. There are trends over various timescales that will affect the observed  $T$  in a different manner at these different geographic

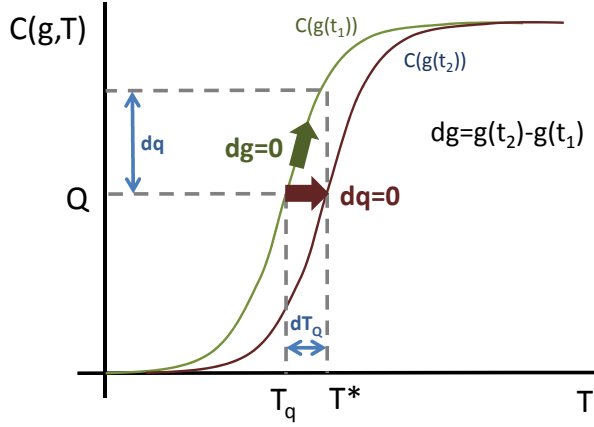


Fig. 1: Temperature  $T_q$  is observed with likelihood  $q$ . If the temperature cdf is not changing with time, ( $g$  is constant) then temperature  $T^*$  is from the same distribution as temperature  $T_q$  and is observed with likelihood  $q + dq$ . This is the path  $dg = 0$ . If the temperature cdf is changing with time, due to forcing  $g(t)$ , then temperature  $T^*$  is observed at time  $t_2$  with the same likelihood  $q$  as temperature  $T_q$  was observed at  $t_1$ . This is the path  $dq = 0$ .

locations. We are interested in developing a technique which isolates the effect of any slow, monotonic trend operating across a long, multidecadal interval. We will assume that this monotonic trend can be associated with an underlying climate forcing which has parameter  $g$ . In what follows we will not need to specify the detailed nature of the relationship between change in  $g$  and in trends in the climate as seen in the changing statistical properties of  $T$ , just that there is such a relationship. An underlying assumption is then that the effect of changing  $g$  on the distribution of observations of  $T$  is on a much longer timescale than that over which individual samples of  $T$  distributions are obtained. For each location we can aggregate daily seasonal temperature observations over some multi-year interval  $\tau$ , centred on time  $t$ , to obtain a cumulative density function (cdf). Let us assume that the cdf  $C(T, g(t))$  can be treated as a continuous function of temperature and of time dependent forcing  $g$ . Then at a given time  $t$  when there is a level of climate forcing  $g(t)$ , the cdf value  $q$  is the likelihood of the quantile  $T_q$  of a given temperature observation  $T \leq T_q$ :

$$C(T_q, g(t)) = q \quad (2.1)$$

$$T_q = \tilde{C}(q, g(t)) \quad (2.2)$$

where  $\tilde{C}$  is the quantile function obtained by inverting the cdf w.r.t. temperature. We can write the variation, to leading order:

$$dq = \left[ \frac{\partial C}{\partial T_q} \right]_g dT_q + \left[ \frac{\partial C}{\partial g} \right]_{T_q} dg \quad (2.3)$$

and

$$dT_q = \left[ \frac{\partial \tilde{C}}{\partial q} \right]_g dq + \left[ \frac{\partial \tilde{C}}{\partial g} \right]_q dg \quad (2.4)$$

At some later time we observe a temperature  $T^*$  so that  $dT_q = T^* - T_q$ . We can in principle ask for the contribution to the observation  $T^*$  in the absence of forcing, that is  $dg = 0$ , directly from the change in the quantile function and from (2.4) this is:

$$dT_q(dg = 0) = \left[ \frac{\partial \tilde{C}}{\partial q} \right]_g dq \quad (2.5)$$

We can also ask for the contribution to the observation  $T^*$  solely due to forcing, that is at  $dq = 0$ , from the quantile function and from (2.4) this is:

$$dT_q(dq = 0) = \left[ \frac{\partial \tilde{C}}{\partial g} \right]_q dg \quad (2.6)$$

This is illustrated in Figure 1. A sufficiently accurate approximation for the quantile function at two times  $t_1$  and  $t_2$  would directly give an estimate of the discrete change  $\Delta T_q$  over an interval  $[t_1, t_2]$ . As  $dT_q \rightarrow \Delta T_q$  we approximate

$$\left[ \frac{\partial \tilde{C}}{\partial g} \right]_q dg \rightarrow \Delta \tilde{C}(q, g(t_2), g(t_1)) \simeq \tilde{C}(q, g(t_2)) - \tilde{C}(q, g(t_1)) \quad (2.7)$$

This direct estimate of the change  $\Delta T_q$  due to climate forcing requires full knowledge of the quantile function, that is, the inverse of the cdf. In practice, given that there is a fundamental upper limit on the number of observations in a given season, this can be problematic, particularly in the tails of the distribution for non-Gaussian processes. We can instead obtain an expression where only a direct estimate of the cdf is needed. Setting  $dq = 0$  in (2.3) we obtain

$$dT_q(dq = 0) = -\frac{1}{P} \left[ \frac{\partial C}{\partial g} \right]_{T_q} dg \quad (2.8)$$

where  $P(T_q, g(t))$  is the probability density function (pdf). Now let us compare two different realizations of the cdf obtained at different times  $t_1$  and  $t_2$  over which there is the discrete change  $\Delta T_q$ . Then, as  $dT_q \rightarrow \Delta T_q$  we approximate

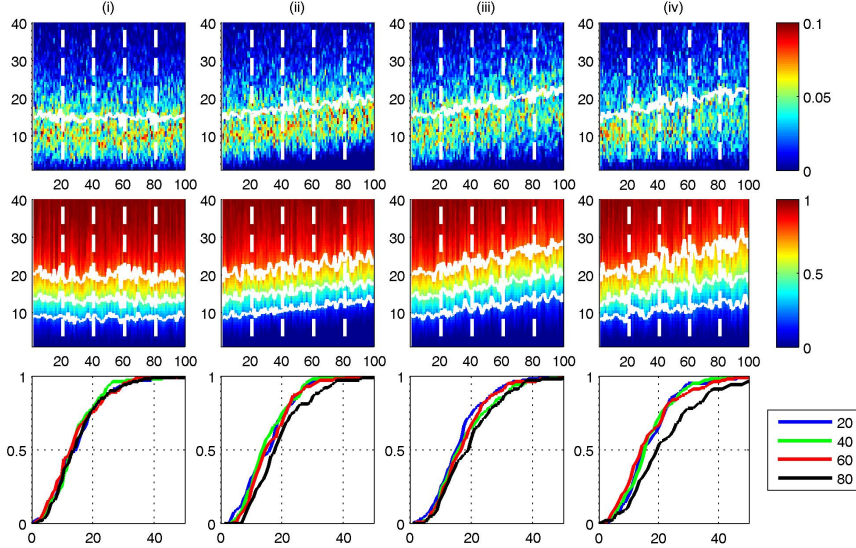


Fig. 2: Pseudo annual temperature data with (i) no time variation (ii) constant shift at all temperatures (iii) mean and variance increase with time and (iv) mean, variance, skew and kurtosis increase with time. Panels show from top to bottom: 'yearly' (100 sample) pdfs with temperature as ordinate and time as abscissa and a solid white line indicating the mean; 'yearly' (100 sample) cdfs, same axes, solid white lines indicating the 0.25, 0.5 and 0.75 quantiles; the vertical dashed white lines indicate four 'years' for which four individual cdfs are plotted in mid panels with temperature as abscissa.

$$\left[ \frac{\partial C}{\partial g} \right]_{T_q} dg \rightarrow \Delta C(T_q, g(t_2), g(t_1)) \simeq C(T_q, g(t_2)) - C(T_q, g(t_1)) \quad (2.9)$$

then

$$\Delta T_q(dg=0) \simeq -\frac{\Delta C}{P} \quad (2.10)$$

This expression suggests pragmatic strategies for estimating a *sensitivity parameter*  $S = \Delta T_q(dg=0)$ . This parameter is a function of the observed variable, here temperature  $T$ , and of the geographical location at which  $T$  is observed. It parameterizes which parts of the distribution that are changing most rapidly with forcing  $g$ . We can immediately see that the pdf acts as an amplification factor for sensitivity. A given change in cdf will be most impactful where the pdf is small, that is, in the tails of the distribution rather than at the mean.

### 3. Illustration with model data

We first illustrate the method, and how it can be used to optimise against observational statistical uncertainty by constructing a test time-series of 'temperature observations' as follows. We have daily observations over a 'season' which is typically no longer than 3 months, over a period of typically 50-100 years. For each 'year' of the test time-series we then select a sample of 100 independent, identically distributed random numbers that are Gamma distributed, with pdf:

$$P(x, t) = \frac{1}{b(t)^{a(t)} \Gamma(a(t))} x^{a(t)-1} e^{-\frac{x}{b(t)}} \quad (3.1)$$

For each 'year'  $t$ , that is, each 100 element sample, we specify the shift and scale parameters  $a(t)$  and  $b(t)$ . These determine the mean ( $ab$ ) the variance, ( $ab^2$ ), the skewness ( $2/\sqrt{b}$ ) and the excess Kurtosis ( $6/b$ ). To model a distribution with slowly changing forcing  $g(t)$  we will consider a linear change in  $a$  and/or  $b$  from one 'year' to the next.

Figure 2 shows 100 'years' of this pseudo- temperature data. The column (i) is for 100 samples ('years') with the same constant  $a = a_0 = 3$  and  $b = b_0 = 5$ , representing a time series with no underlying change in forcing  $g(t)$ . The column (ii) is the same samples but with each shifted such that  $x \rightarrow x + 5 \times t/100$ ; this is a uniform shift across the entire distribution. The column (iii) has  $b$  constant and  $a(t) = a_0[1 + 1/2(t/100)]$  so that the mean and variance both increase with increasing years  $t$  and column (iv) has  $a$  constant and  $b(t) = b_0[1 + 1/2(t/100)]$  so that the first four moments all increase with increasing years  $t$ . The top panel shows the 'yearly' pdfs with the mean indicated by a white line, the second from top panel shows the 'yearly' cdfs, with 0.25, 0.5 and 0.75 quantiles indicated by white lines. The four vertical dashed lines, at  $t = [20, 40, 60, 80]$  indicate the years for which cdfs are plotted in the third panel from the top. The pseudo-temperature series has an approximately linear trend in these quantiles.

Clearly there is considerable statistical variation in the pdfs, and to a lesser extent, the cdfs, as a consequence of small yearly sample size. To increase the sample size we need to aggregate observations over several consecutive years. Our expression (2.10) allows us to optimize this separately for the pdf and the cdf. A procedure for this is shown in Figure 3. The top two rows of panels show the same time-series as Figure 2, but now the pdfs and cdfs are of aggregates over 3 (Figure 3(a)) and 9 (Figure 3(b)) years respectively, the abscissa now indicates the central year of each aggregate. The set of four individual cdfs now show trends which are particularly clear in the 9 year aggregate cdfs; in our simple model for a temperature time-series we can see that a roughly linear positive trend in the mean and variance of a pdf with non zero skew leads to the largest change in the positive upper quadrant of the cdf, rather than at the mean. If the skew and kurtosis also have a positive trend the largest change in the cdf moves further to large positive values.

The bottom two rows of panels of Figures 3(a) and (b) refer to the indirect estimation of the sensitivity from expression (2.10) above. To estimate the pdf, we have aggregated over the entire set of samples, that is, the full dataset. The difference  $\Delta C$  is taken between the cdfs estimated from samples centred on  $t = 80$  and  $t = 20$ . These samples for each of the pair of cdfs are over (Figure 3(a))  $\tau = 3$

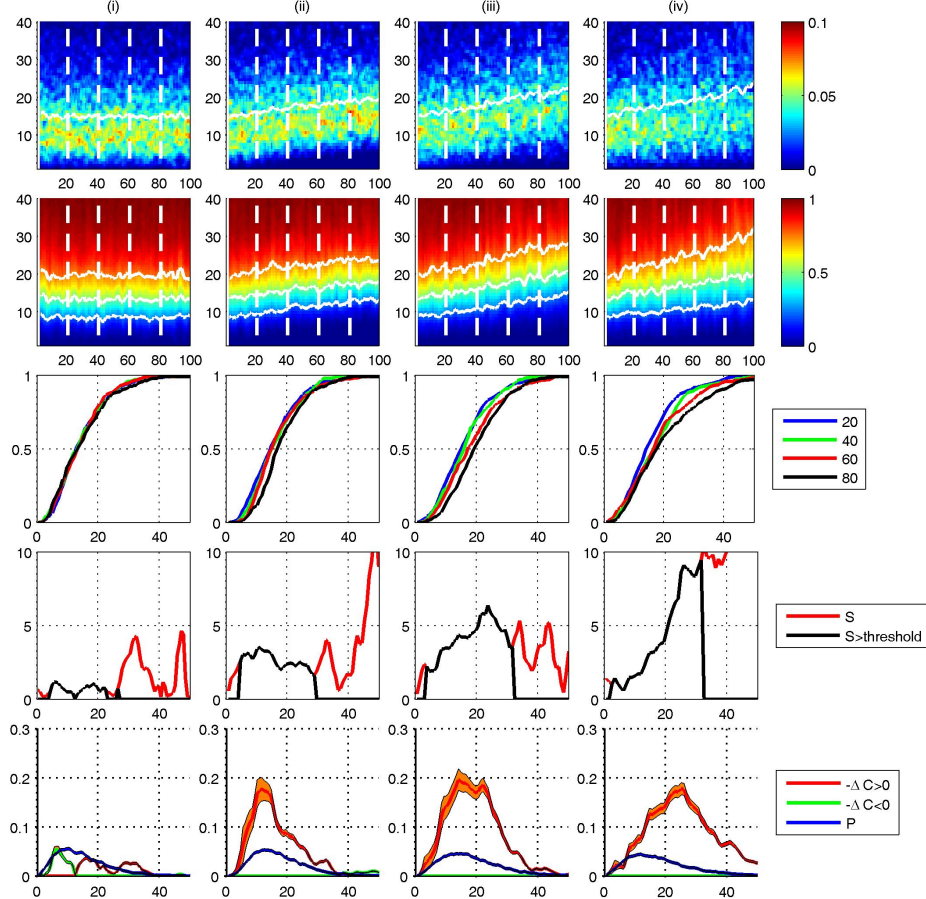


Fig. 3(a): Pseudo annual temperature data, (i)-(iv) and top 3 rows are as the previous figure except that the pdfs and cdfs are  $\tau = 3$  'year' aggregates (300 samples). Lower 2 panels show: sensitivity with temperature as abscissa (red line), and values exceeding a threshold (black line); pdf from aggregate over the entire dataset (blue line) and  $-\Delta C$  (orange line) and  $+\Delta C$  from the 3 year aggregates.

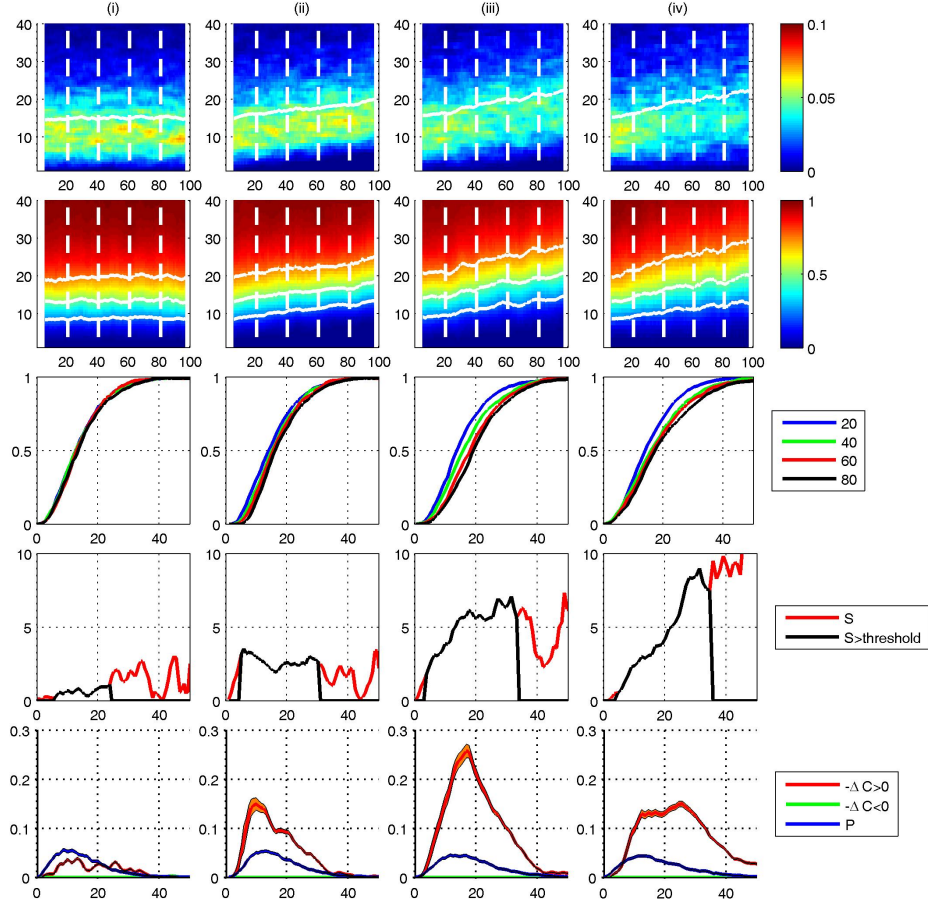


Fig. 3(b): Pseudo annual temperature data, as per previous figure except with  $\tau = 9$  year aggregates.

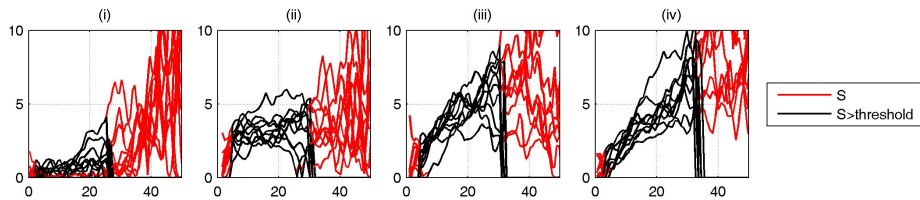


Fig. 4(a): Indirect estimate of sensitivity for 10 realizations of pseudo annual temperature data with 3 year aggregates used to estimate the cdf. The model data parameters (i)-(iv) are as in previous figures.

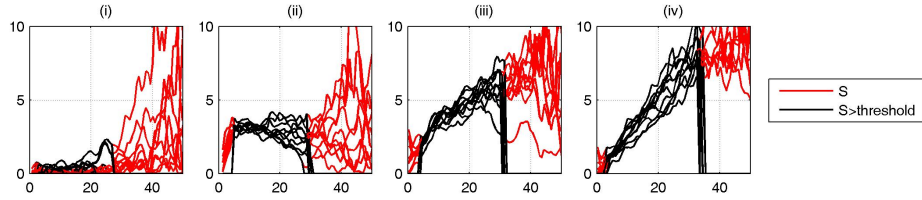


Fig. 4(b): Indirect estimate of sensitivity for 10 realizations of pseudo annual temperature data with 9 year aggregates used to estimate the cdf. The model data parameters (i)-(iv) are as in previous figures.

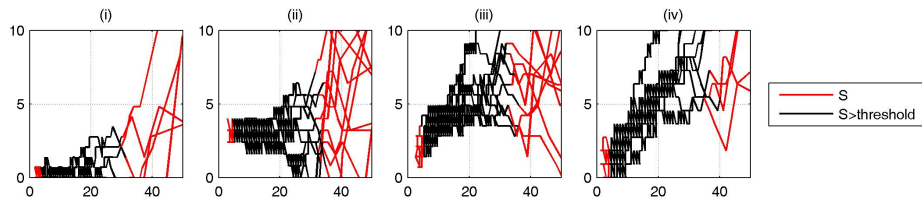


Fig. 5(a): Direct estimate of sensitivity for 10 realizations of pseudo annual temperature data with 3 year aggregates used to estimate the cdf. The model data parameters (i)-(iv) are as in previous figures.

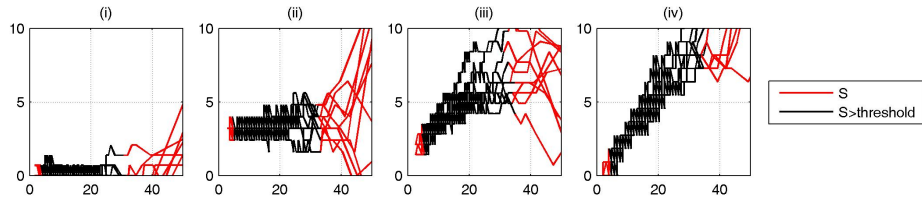


Fig. 5(b): Direct estimate of sensitivity for 10 realizations of pseudo annual temperature data with 9 year aggregates used to estimate the cdf. The model data parameters (i)-(iv) are as in previous figures.

and (Figure 3(b))  $\tau = 9$  'years' respectively. These are plotted in the bottom panel, with uncertainties, indicated by shading, estimated as  $\sqrt{(m)}$  where  $m$  is the number of samples per pdf histogram bin.

In the panel above, the ratio  $S = -\Delta C/P$  obtained from these is plotted (red line) for all values. Clearly, when either  $-\Delta C$  or  $P$  is small, this ratio is dominated by statistical uncertainty and we have overplotted (black line) values where the magnitude of both  $\Delta C$  and  $P$  exceed a threshold value of 0.01. For arbitrarily good statistics, these plots should show the following, from left to right: column (i)  $\Delta C \rightarrow 0$ , so  $S \rightarrow 0$ , (ii)  $S$  constant (iii), and to a greater extent (iv)  $S$  is largest for values of  $x$  greater than the mean as the +ve skew and Kurtosis both increase with  $t$ .

Increasing the sample interval  $\tau$  over which the cdfs used to obtain  $\Delta C$  are estimated improves statistics. This procedure is valid provided that this interval  $\tau$  is much shorter than that over which  $g(t)$  is changing. Importantly in real data, this procedure effectively removes trends on timescales shorter than  $\tau$ . We demonstrate this using the pseudo-temperature data in Figures 4 (a) and (b) for  $\tau = 3$  and  $\tau = 9$  'years' respectively. In these plots we calculate the sensitivity  $S$  for 10 successive realizations of the pseudo-temperature data, that is, we increment  $t_1$  and  $t_2$  by one year for each curve that is plotted, keeping the interval  $t_2 - t_1$  fixed. For arbitrarily large sample size these curves should collapse on top of each other. This suggests an operational measure for the reliability of the sensitivity; one can consider a given value of sensitivity to be reliable provided that value is exceeded in all (here 10) realizations. A further check on the robustness of the trend in time is to construct a surrogate dataset, (see also [4]) that is, to recalculate the sensitivity having randomly shuffled the time order in which the samples are observed; this quantifies the observed sensitivity that could occur randomly with these finite sample statistics.

We finally compare this method with direct estimation of the sensitivity using expression (2.6). This is shown in Figures 5 (a) and (b) which are in the same format as figures 4 (a) and (b) but where we have numerically inverted the cdf to obtain the quantile function. We plot the difference in quantile function with all values are plotted as a red line, and values for  $0.05 < C < 0.95$  plotted as a black line. We can see that the indirect method and direct methods correspond within errors; the discretization or 'stepping' in Figure 5 is a direct consequence of the process of numerical inversion of the cdf.

#### 4. Application: eObs temperature data

We now illustrate this methodology with daily temperature measurements from the E-OBS gridded dataset [10] [1950-2011 v5.0]. We will look at four locations at longitude and latitude (i) [4.75 52.25] Leiden Holland (ii) [-4.75 51.75] west Wales (iii) [-4.75 42.75] Leon, north Spain (iv) [11.25 43.75] Florence, Italy. We will repeat the above procedure using data from these four locations, focussing on summer aggregating daily temperatures over 3 month intervals within each year of observation, June, July and August, giving a sample of 92 observations per year.

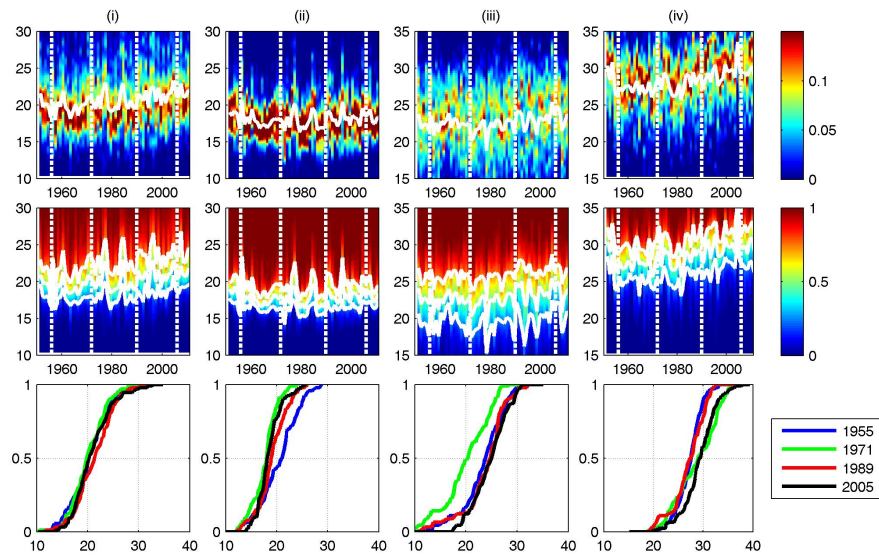


Fig. 6: Eobs annual temperature data at four locations (i) - (iv). Panels show from top to bottom: yearly summer (92 sample) pdfs with temperature as ordinate and time as abscissa and a solid white line indicating the mean; 'yearly' (92 sample) cdfs, same axes, solid white lines indicating the 0.25, 0.5 and 0.75 quantiles; the vertical dashed white lines indicate four years for which four individual cdfs are plotted in mid panels with temperature as abscissa.

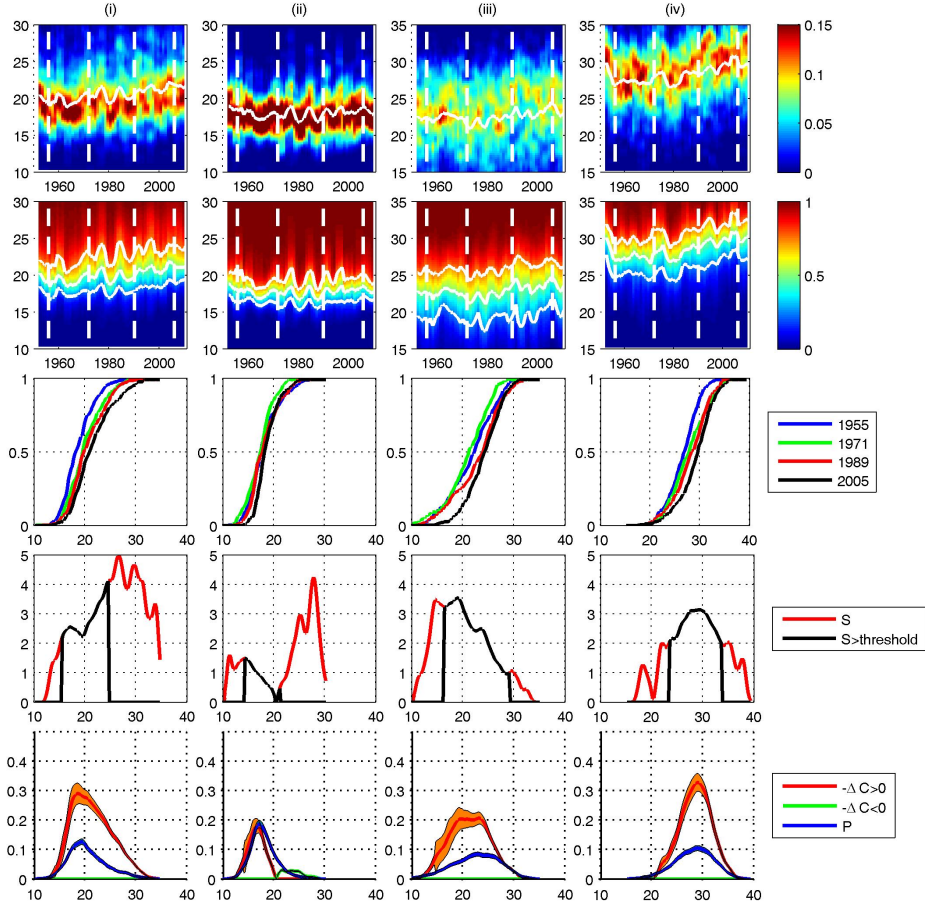


Fig. 7(a): E-Obs temperature data, for four locations (i)-(iv) in the same format as Figure 3 with  $\tau = 3$  year aggregates.

Figure 6 shows the pdfs and cdfs for these yearly samples in the same format as Figure 2. Figures 7(a) and (b) are in the same format as figures 3 (a) and (b) showing the data with sample  $\tau = 3$  and 9 years respectively; here  $\Delta C$  is estimated using samples centred on years 1955 and 2005 and as above, the pdf is estimated from the entire dataset.

Distinct behaviour can be seen at these four locations. Holland (i) shows a clear skew towards higher temperatures and which peaks at the largest temperatures. West Wales (ii) shows no significant sensitivity. North Spain shows similar sensitivity across the distribution and Florence is sensitive across the distribution, but maximally and uniformly above the 0.5 quantile.

Figures 8 (a) and (b) show the sensitivity estimated for 10 successive intervals in the same manner as above; that is,  $\Delta C$  is estimated using samples centred on years  $t_1 = 1955 - 1965$  and  $t_2 = 1995 - 2005$  with the same  $t_2 - t_1$  for all the curves. Here there is both variability due to the finite size of the sample as seen in

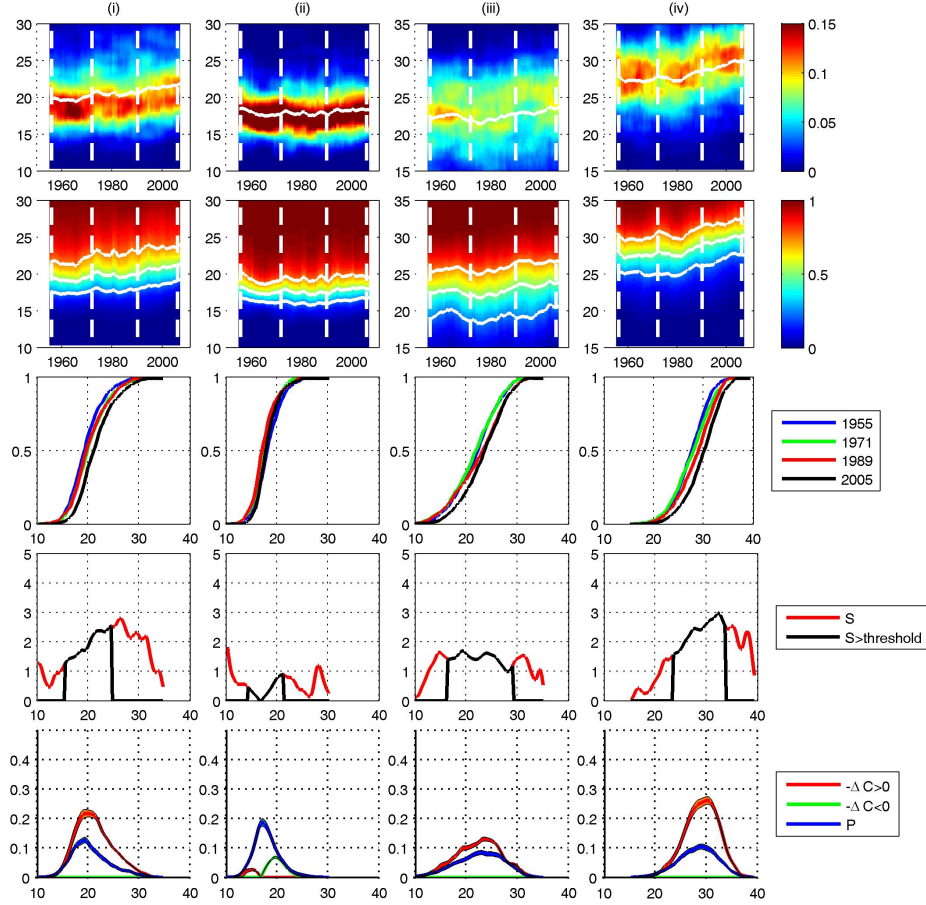


Fig. 7(b): E-Obs temperature data, as per previous figure except with  $\tau = 9$  year aggregates.

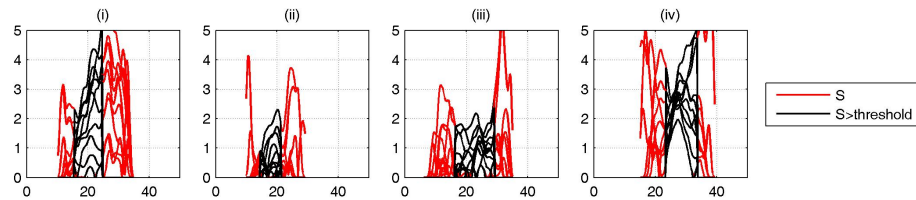


Fig. 8(a): Indirect estimate of sensitivity for 10 realizations of eObs temperature data with 3 year aggregates used to estimate the cdf. The locations (i)-(iv) are as in previous figures.

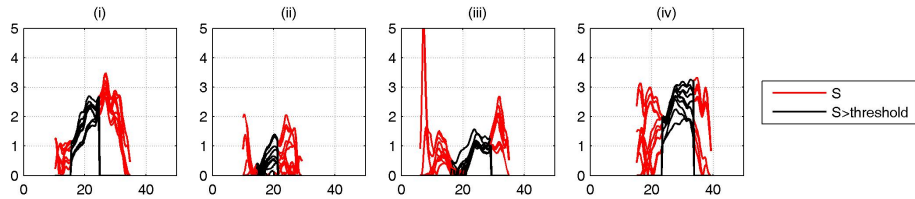


Fig. 8(b): Indirect estimate of sensitivity for 10 realizations of eObs temperature data with 9 year aggregates used to estimate the cdf. The locations (i)-(iv) are as in previous figures.

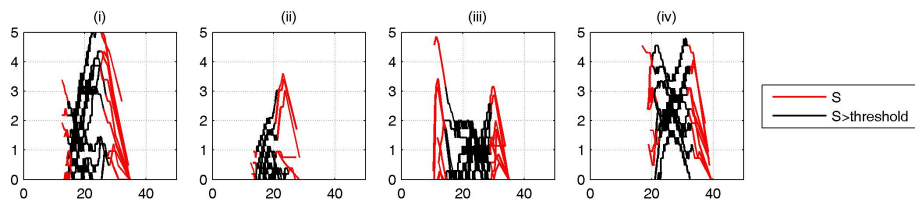


Fig. 9(a): Direct estimate of sensitivity for 10 realizations of eObs temperature data with 3 year aggregates used to estimate the cdf. The locations (i)-(iv) are as in previous figures.

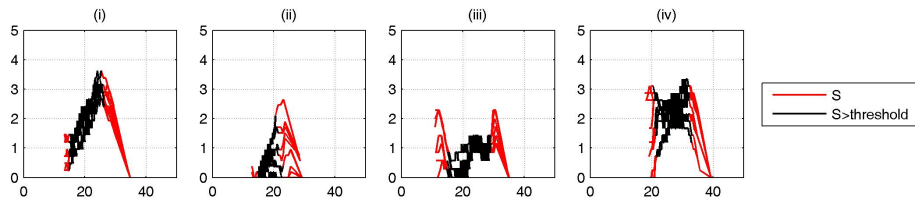


Fig. 9(b): Direct estimate of sensitivity for 10 realizations of eObs temperature data with 9 year aggregates used to estimate the cdf. The locations (i)-(iv) are as in previous figures.

the model data above, and in addition systematic trends due to departures from our simple assumption (2.10).

Finally, we have recalculated the curves of Figure 8 (a) and (b) using the direct estimate of sensitivity (2.6) and these are shown in Figures 9 (a) and (b). Again, within uncertainties, these track the behaviour seen in Figure 8 (a) and (b).

## 5. Conclusions

We have presented a method which provides an improved way of understanding the observed consequences of a globally changing climate at specific locations and for specific thresholds. It provides a methodology for informing user specific decisions which are often vulnerable to specific thresholds. It avoids the use of complicated models and all the epistemic uncertainties which that can involve. There are further interesting mathematical challenges in applying it to different types of distributions such as those representing precipitation, multi-variable distributions and functions of multiple variables. There are also, of course, opportunities to apply the method to thresholds experienced in real-world situations. These could be as diverse as building design, infrastructure vulnerability, strategic planning for heat waves, changing risks of crop failure and impacts on food prices etc. These opportunities are intrinsically multi-disciplinary in nature and provide an exciting and rich vein of new research opportunities to support science based policy and decision making.

## Appendix: Return times

The above formalism is directly related to the return time of events. In time period  $\Delta t$  we observe  $N$  events which in ascending size order are  $x_1 \dots x_k \dots x_N$  and have a mean time between observations of  $\delta t = \Delta t/N$ . Then within period  $\Delta t$  there are  $N - k + 1$  events of size  $x \geq x_k$ . The return period or return time  $R$  for an event 'at least as big as  $x = x_k$ ' is then (see also [11]):

$$R(x) = \frac{\Delta t}{(N - k + 1)} \simeq \frac{\Delta t}{(N - k)} \quad (\text{A.1})$$

for  $(N - k)$  large. In this large  $(N - k)$  limit, the cdf  $C(x = x_k) = k/N$  so that:

$$R(x) = \frac{\delta t}{(1 - C(x))} \quad (\text{A.2})$$

Note that the return time is only sharply defined for sufficiently large  $(N - k)$  if the underlying statistics were Gaussian, then the % error is  $\sim 1/\sqrt{(N - k)}/100$ . Practically, it fails at the largest events  $k \rightarrow N$ .

Now consider the slowly driven system with cdf  $C(x, g(t))$ , there will be a corresponding return time  $R(x, g(t))$ . The changes with  $x$  and  $g$  are:

$$\frac{\partial R(x, g)}{\partial g} = \frac{R}{(1 - C(x, g))} \frac{\partial C(x, g)}{\partial g} \quad (\text{A.3})$$

$$\frac{\partial R(x, g)}{\partial x} = \frac{R}{(1 - C(x, g))} \frac{\partial C(x, g)}{\partial x} \quad (\text{A.4})$$

If we define the change in return time due to change in  $g$  the same manner as  $\Delta C$  above, so that

$$\Delta R = \frac{\partial R}{\partial g} dg \simeq R(x, g(t_2)) - R(x, g(t_1)) \quad (\text{A.5})$$

then using (A.2)

$$\Delta R = \frac{R}{(1 - C)} \Delta C \quad (\text{A.6})$$

Since from above the sensitivity  $dx(dq=0) = -(1/P)(\partial C/\partial g) = -\Delta C/P$  we can express sensitivity in terms of the change in the return time due to change in  $g$ :

$$dx(dq=0) = \frac{(C-1)}{P} \frac{\Delta R}{R} \quad (\text{A.7})$$

Finally, we can check that  $\Delta R$  is indeed the change in return time due solely to change in forcing. The return time is  $T_x = R(x, g)$  with variation:

$$dT_x = \left[ \frac{\partial R}{\partial x} \right]_g dx + \left[ \frac{\partial R}{\partial g} \right]_x dg \quad (\text{A.8})$$

and we have

$$dq = \left[ \frac{\partial C}{\partial x} \right]_g dx + \left[ \frac{\partial C}{\partial g} \right]_x dg \quad (\text{A.9})$$

Now the change in return time due to change in forcing  $g$  only is that at  $dq=0$ . From (A.3) we can see that  $dq=0$  is  $dt_x=0$ ; the total variation in return time is zero. However, the change in return time due to change in forcing alone is, at  $dt_x=0$

$$\Delta R = \left[ \frac{\partial R}{\partial g} \right]_x dg = - \left[ \frac{\partial R}{\partial x} \right]_g dx \quad (\text{A.10})$$

which using (A.3) is just

$$\frac{\partial R}{\partial x} dx = \frac{R}{(1 - C)} \frac{\partial C(x, g)}{\partial x} dx \quad (\text{A.11})$$

which at at  $dq=0$  is just

$$\Delta R = - \frac{R}{(1 - C)} \frac{\partial C(x, g)}{\partial g} dg = \frac{R}{(1 - C)} \Delta C \quad (\text{A.12})$$

as above.

### Acknowledgment

SCC acknowledges support from the EPSRC and STFC. DAS acknowledges the support of the Centre for Climate Change Economics and Policy funded by the ESRC and Munich Re. We acknowledge the E-OBS dataset from the EU-FP6 project ENSEMBLES (<http://ensembles-eu.metoffice.com>) and the data providers in the ECA & D project (<http://eca.knmi.nl>)

### References

- [1] Knutti R, Hegerl GC. The equilibrium sensitivity of the Earth's temperature to radiation changes. *Nature Geosci.* [10.1038/ngeo337]. 2008;1(11):735-43.
- [2] Oreskes N, Stainforth DA, Smith LA. Adaptation to Global Warming: Do Climate Models Tell Us What We Need to Know? *Philosophy of Science*, Vol. 77, No. 5 2010 pp. 1012-1028
- [3] Milly PCD, Betancourt J, Falkenmark M, Hirsch RM, Kundzewicz ZW, Lettenmaier DP, et al. Stationarity Is Dead: Whither Water Management? *Science*. 2008 February 1, 2008;319(5863):573-4.
- [4] Theiler et al, Testing for nonlinearity in time series: the method of surrogate data, *Physica D*, 58, 77, 1992
- [5] Stainforth DA, Allen MR, Tredger ER, Smith LA. Confidence, uncertainty and decision-support relevance in climate predictions. *Philosophical Transactions of the Royal Society a-Mathematical Physical and Engineering Sciences*. 2007 Aug;365(1857):2145-61.
- [6] Stainforth DA, Downing TE, Washington R, Lopez A, New M. Issues in the interpretation of climate model ensembles to inform decisions. *Philosophical Transactions of the Royal Society a-Mathematical Physical and Engineering Sciences*. [Article]. 2007 Aug;365(1857):2163-77.
- [7] McWilliams JC. Irreducible imprecision in atmospheric and oceanic simulations. *Proceedings of the National Academy of Sciences of the United States of America*. 2007;104(21):8709-13.
- [8] Smith LA. What might we learn from climate forecasts? *Proceedings of the National Academy of Sciences of the United States of America*. [Proceedings Paper]. 2002 Feb;99:2487-92.
- [9] Stainforth DA, Chapman SC, Watkins NW. Adaptation Relevant Climate Sensitivity In preparation.
- [10] Haylock, M.R., N. Hofstra, A.M.G. Klein Tank, E.J. Klok, P.D. Jones and M. New. 2008: A European daily high-resolution gridded dataset of surface temperature and precipitation. *J. Geophys. Res (Atmospheres)*, 113, D20119, doi:10.1029/2008JD10201
- [11] Gilchrist, W., Statistical Modelling with Quantile Functions, CRC, 2000